Kinetic and Equilibrium Study on the Axial-Ligand Substitution Reaction of the Head-to-Tail α-Pyridonate-Bridged *cis*-Diammineplatinum(III) Dinuclear Complex: *trans* Effect of the Axial Ligand through the Pt−Pt Bond to the Opposite Axial Ligand

Nami Saeki,[a] Yuji Hirano,[a] Yasunari Sasamoto,[a] Ichiro Sato,[a] Tsuyoshi Toshida,[a] Sousei Ito,[a] Noriko Nakamura,[a] Koji Ishihara,*[a] and Kazuko Matsumoto*[a]

Keywords: Platinum / Pt^{III} dimer / Kinetics / Reaction mechanisms / α-Pyridone

Acid dissociation constant of the axial aqua ligand in the Head-to-Tail (HT) α-pyridonate-bridged *cis*-diammineplatinum(III) dimer complex $\{[(H_2O)Pt(NH_3)_2(\mu\text{-}C_5H_4NO)_2Pt(NH_3)_2(H_2O)]^{4+}\}$ was determined spectrophotometrically to be $-\log(K_{h1}/M) = 1.98\pm0.01$ at 25 °C and $I = 2.00$ M. Successive substitution reaction of the HT dimer with halide ions X^- (X^- = Cl^- and Br^-) at the two axial sites to give monohalo and dihalo complexes was studied kinetically:

$[(H_2O)Pt(NH_3)_2(\mu\text{-}C_5H_4NO)_2Pt(NH_3)_2(H_2O)]^{4+} + X^- \rightleftarrows$
$[(H_2O)Pt(NH_3)_2(\mu\text{-}C_5H_4NO)_2Pt(NH_3)_2(X)]^{3+} + H_2O$ (k_{obs1})
$[(H_2O)Pt(NH_3)_2(\mu\text{-}C_5H_4NO)_2Pt(NH_3)_2(X)]^{3+} + X^- \rightleftarrows$
$[(X)Pt(NH_3)_2(\mu\text{-}C_5H_4NO)_2Pt(NH_3)_2(X)]^{2+} + H_2O$ (k_{obs2})

Formation constants of the monohalo and dihalo complexes were determined spectrophotometrically to be $\log(K_1^{Cl}/M^{-1}) = 5.27\pm0.02$ and $\log(K_2^{Cl}/M^{-1}) = 3.83\pm0.01$ for the reaction with Cl^-, and $\log(K_1^{Br}/M^{-1}) = 5.33\pm0.03$ and $\log(K_2^{Br}/M^{-1}) = 4.44\pm0.02$ for the reaction with Br^-. In the HT dimer having two equivalent platinum atoms, the deprotonation occurs to the water molecule on one of the two Pt atoms, whereas the first nucleophilic substitution with X^- occurs to the other Pt atom. Substitution of the second water ligand with Cl^- proceeds by a simple substitution path, whereas the second substitution with Br^- proceeds by two parallel paths: one includes the dissociation of the axially coordinated water molecule followed by the Br^- coordination, and the other is the simple one-step substitution path. The difference of the reaction paths is reasonably explained by the different *trans* effect of the halide ions exerted through the Pt–Pt bond to the other terminal Pt atom in the monohalo complexes.

Introduction

There are a substantial number of diplatinum(III) complexes that involve metal−metal bonding between two d^7 platinum atoms.[1−10] They are classified into two groups: the first group involves symmetrical bridging ligands with identical coordinating atoms at both ends of the bridge, such as pyrophosphate-*P,P*, sulfate-*O,O*, and hydrogen phosphate-*O,O* ligands, and the complexes have the "lantern" structure with four symmetrically bridging ligands. The second group, which we will deal with in this report, involves complexes having asymmetrical bridging ligands with different coordinating atoms, such as α-pyrrolidonate-*N,O*, α-pyridonate-*N,O*, and acetamidate-*N,O*. These bridging ligands also appear in a class of multinuclear mixed-valent complexes called "platinum blues".[11−20] The complexes in the second group, Head-to-Head (HH) dinuclear Pt^{III} complexes $[Pt_2(NH_3)_4(N^{\cap}O)_2(X)_2]^{n+}$ ($N^{\cap}O$ = amidate, X = NO_3^-, NO_2^-, H_2O, or Cl^-, n = 2 or 4) are formed by the oxidation of "platinum blues". The two platinum atoms in the HH form are not equivalent, as shown by Scheme 1. The other isomer, head-to-tail (HT) is also known for this class of compounds, however isomerization between HH and HT of the Pt^{III} dimers does not occur in aqueous solution. The HH to HT or vice versa isomerization takes place only for the Pt^{II} dimer complexes.

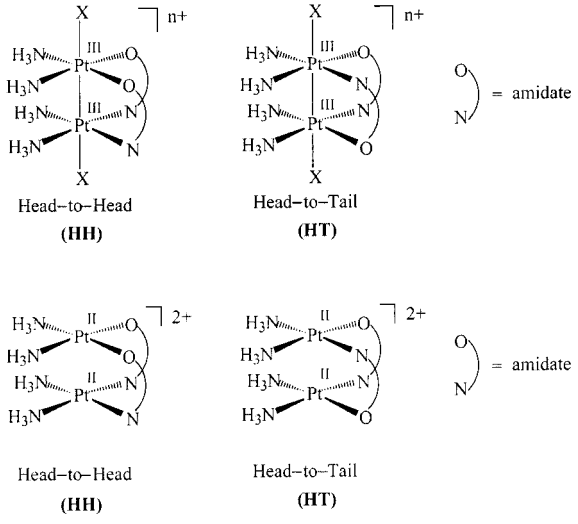

Scheme 1

As an exception, an isomerization reaction has been reported for the Pt^{III} dimer complex HH-$[Pt_2^{III}(CH_3)_4$(2-hy-

[a] Department of Chemistry, School of Science and Engineering, Waseda University,
Okubo, Shinjuku-ku, Tokyo 169−8555, Japan
Fax: (internat.) +81-3-3208-2735
E-mail: ishi3719@mn.waseda.ac.jp and
kmatsu@mn.waseda.ac.jp

Supporting information for this article is available on the WWW under http://www.wiley-vch.de/home/eurjic or from the author.

  1434−1948/01/0808−2081 $ 17.50+.50/0

droxy-6-fluoropyridonato)$_2$Py], which isomerizes to the head-to-tail (HT) isomer, HT-[$Pt_2^{III}(CH_3)_4$(2-hydroxy-6-fluoropyridonato)$_2$(Py)$_2$], when the former reacts with pyridine in chloroform.[21] Such HH to HT isomerization has been reported for several Pt^{II} dimer complexes with similar bridging amidate ligands,[22] but for Pt^{III} dimer complexes, the above-mentioned reaction represents the only example of this isomerization reported so far. Unlike their reduced forms, i.e., the Pt^{II} dimers $[Pt_2(NH_3)_4(N^{\cap}O)_2]^{2+}$, the Pt^{III} dimer complexes have axial ligands at both ends of the Pt−Pt axis, and these axial ligands play an important role in determining the chemical properties of the complex in solution. In spite of this fact, there are few kinetic studies on the axial ligand substitution reactions for the Pt^{III} dimer complexes; only a few kinetic studies have been reported for Pt^{III} dimers of the first group,[23,24] and even the reports on the simplest yet fundamentally important equilibrium parameters such as the acidity constant of the axially coordinated water are limited.[8,25]

In this paper we report the kinetic and equilibrium study on the axial aqua ligand substitution by halide ligands on the HT α-pyridonate-bridged Pt^{III} dinuclear complex, HT-$[(H_2O)Pt(NH_3)_2(\mu\text{-}C_5H_4NO)_2Pt(NH_3)_2(H_2O)]^{4+}$. Halide ions were selected as ligands rather than NO_2^-, SO_4^{2-}, etc., in order to avoid the problem of so-called "proton ambiguity" in kinetics,[26] since the dinuclear Pt^{III} complexes are found to be hydrolyzed even in highly acidic aqueous solution.

Results and Discussion

Preliminary ^{1}H NMR measurements were done, as is shown in Figure 1. When a small amount of Cl^- was added to the HT dimer solution, new peaks appeared at δ = 8.15 and 8.63 (Figure 1, b and c). Another peak was enhanced at δ = 8.7 with a decrease of the peaks at δ = 8.15 and 8.63, as [Cl^-] was increased. The peaks at δ = 8.15 and 8.63, and δ = 8.7 are assigned to the monochloro and dichloro complexes, respectively, and show that only one monochloro complex is formed and is converted to the dichloro complex.

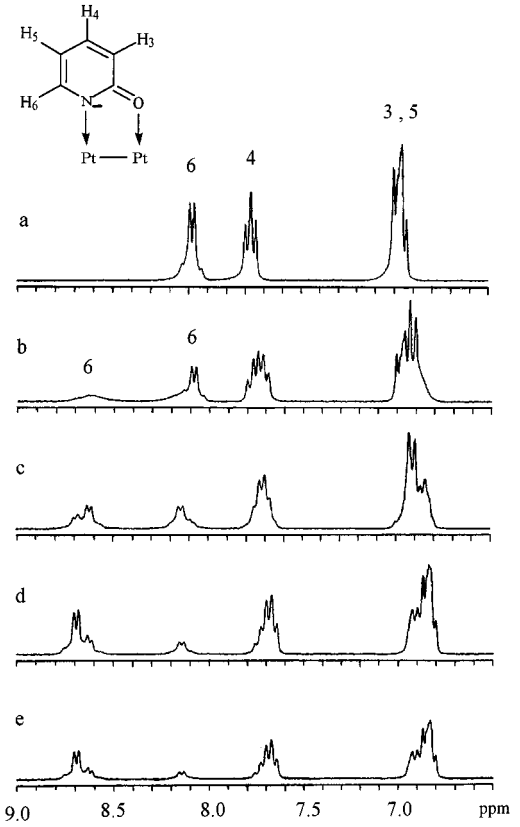

Figure 1. The ^{1}H NMR spectra of the HT dimer in acidic D_2O solution with different C_{Cl^-} at room temperature; [$DClO_4$] = 1.3 M, [HT] = 1.9×10^{-2} M, [Cl^-]/[HT] = 0 (a), 0.5 (b), 1.0 (c), 1.5 (d), 2.0 (e); solid began to precipitate at (d)

Acid Dissociation Constant of the HT Dimer

The X-ray crystallography study shows[4] that two nitrate ions cap axial positions of the HT-[$Pt_2^{III}(NH_3)_4$(α-pyridonato)$_2$(NO_3)$_2$]$^{2+}$ in solid state. Both axial nitrate ions are completely replaced by H_2O or OH^- on dissolution, since no spectral change was observed when sodium nitrate was added up to 0.020 M (mol dm^{-3}) to the aqueous solutions of the HT dimer (5.0×10^{-5} M). When the acidity of the solution was varied, an isosbestic point was observed at 244 nm (Figure SI-1, see Supporting Information). The HT dimer is stable in strongly acidic aqueous solution, and no decomposition was observed by acidification at least for several hours. The spectral change (Figure SI-1, see Supporting Information) is pH-dependent and the change can be reversed by pH adjustment. The spectral change corresponds to deprotonation of the coordinated axial water molecule as expressed in Equation (1). The deprotonation occurs to either one of the two equivalent water molecules in the HT isomer.

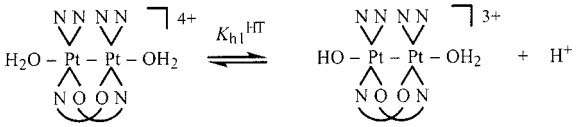

(1)

$[H_2O{-}Pt(N_3O){-}Pt(N_3O){-}OH_2]^{4+}[HO{-}Pt(N_3O){-}Pt(N_3O){-}OH_2]^{3+}$

The apparent molar absorption coefficient ε is expressed as $\varepsilon = (\varepsilon_1 + \varepsilon_2 K_{h1}[H^+]^{-1})(1 + K_{h1}[H^+]^{-1})^{-1}$, where ε_1 and ε_2 are the molar absorption coefficients of the undissociated dimer $H_2O{-}Pt(N_3O){-}Pt(N_3O){-}OH_2$ and the deprotonated dimer $H_2O{-}Pt(N_3O){-}Pt(N_3O){-}OH$, respectively, and K_{h1} is the first acid dissociation constant of the diaqua complex. The ε values at 250, 255, 260, 270, and 280 nm were analyzed simultaneously as a function of [H^+] by using a nonlinear least-squares fitting method. The K_{h1} values obtained at I = 2.00 M are as follows: $-\log(K_{h1}/M)$ = 1.98±0.01 (25.0 °C), 1.68±0.02 (35.0 °C). The value of K_{h1} for the present HT dimer is more than 1 order of magnitude larger than that of the related Pt^{III} dimer complex with dif-

ferent bridging ligands: $-\log(K_{h1}/M) = 3.49$ for the 1-methyluracilate-bridged HT dimer.[8] This difference can be explained by the less-donating α-pyridonate coordination, as compared to methyluracilate. Because of the weaker donation, the Pt^{III} atom in the α-pyridonate complex would be more electron withdrawing.

Formation Constants of the Monohalo and Dihalo Complexes

The absorption spectra were measured at $I = 2.00$ M, $[H^+] = 1.27$ M, and 25 °C, under various C_X^-/C_{HT} for a fixed C_{HT}. The results are shown in Figure 2 for both reactions with Cl^- and Br^-, in which two distinct isosbestic points are observed at 251 and 273 nm, and at 256 and 295.5 nm, respectively.

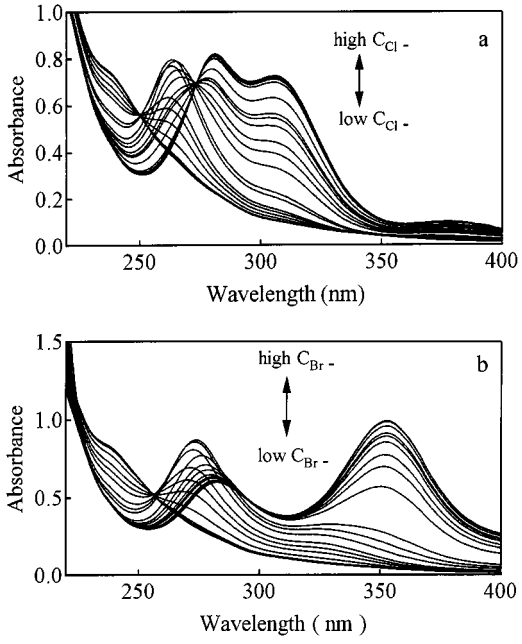

Figure 2. The UV/Vis spectra of the HT dimer in acidic aqueous solution with different C_{Cl}^- (a) and C_{Br}^- (b) at 25 °C and $I = 2.00$ M. $[H^+] = 1.27$ M; $C_{Cl}^- = (0-1.35) \times 10^{-2}$ M (a); $C_{Br}^- = (0-1.20) \times 10^{-2}$ M (b); $C_{HT} = 2.5\times10^{-5}$ M (a), 2.8×10^{-5} M (b)

Plots of the absorbance at the isosbestic point of the longer wavelength (273 nm, 295.5 nm) against C_X^-/C_{HT} showed a clear inflection point at $C_X^-/C_{HT} = 1$, however, another inflection point corresponding to $C_X^-/C_{HT} = 2$ was obscured, probably because of the smaller formation constant of the dihalo complex. The formation of the dichloro complex has also been confirmed by X-ray crystallography for the dichloro HH α-pyrrolidonate-bridged dimer,[26] in addition to the ^1H NMR results mentioned above. Therefore, the observed spectral change in Figure 2 corresponds to the following reactions.

$$[(H_2O)Pt(NH_3)_2(\mu\text{-}C_5H_4NO)_2Pt(NH_3)_2(H_2O)]^{4+} + X \xrightleftharpoons{K_1^X} [(H_2O)Pt(NH_3)_2(\mu\text{-}C_5H_4NO)_2Pt(NH_3)_2(X)]^{3+} + H_2O \quad (2)$$

$$[(H_2O)Pt(NH_3)_2(\mu\text{-}C_5H_4NO)_2Pt(NH_3)_2(X)]^{3+} + X \xrightleftharpoons{K_2^X} [(X)Pt(NH_3)_2(\mu\text{-}C_5H_4NO)_2Pt(NH_3)_2(X)]^{2+} + H_2O \quad (3)$$

The K_1^X and K_2^X values were obtained at $I = 2.00$ and 25 °C, by simultaneously analyzing the absorbance at twelve different wavelengths between 235 nm and 305 nm, and are given in Table 1 together with K_{h1} values. The K_1^{Cl} and K_2^{Cl} values are comparable to those reported for the HH α-pyrrolidonate-bridged cis-diammineplatinum(III) dimer with Cl^-.[25]

Table 1. Equilibrium constants for the reaction of the HT α-pyridonate-bridged *cis*-diammineplatinum(III) dimer with halides determined at $I = 2.00$ M ($[H^+] = 1.27$ M) and 25 °C spectrophotometrically

$-\log K_{h1}$ [mol L^{-1}]	$\log K_1^{Cl}$ [L mol^{-1}]	$\log K_2^{Cl}$ [L mol^{-1}]	$\log K_1^{Br}$ [L mol^{-1}]	$\log K_2^{Br}$ [L mol^{-1}]
1.98±0.01	5.27±0.02	3.83±0.01	5.33±0.03	4.44±0.02
3.49[a]				

[a] For HT 1-methyluracilate-bridged *cis*-diammineplatinum(III) dimer.[8]

Kinetics for the Formation of the Monohalo Complexes

Under the conditions of $C_{HT} >> C_X^-$ and $[H^+] = 0.10-0.82$ M, reactions of the HT dimer with X^- were first order and monophasic, i.e., only reaction (2) was observed. The formation rate of the monohalo complex (Pt_2X) is given by Equation (4), where $[X^-]$ is the concentration of the free halide ion. The conditional first-order rate constant, k_{obs1} was found to involve the dimer concentration and $[H^+]$.

$$d[Pt_2X]/dt = k_{obs1}[X^-] \quad (4)$$

Since k_{obs1} was linearly dependent on C_{HT} at a given $[H^+]$ as shown in Figure 3 (a), k_{obs1} is expressed as Equation (5), where k_{f1} is the second order rate constant.

$$k_{obs1} = k_{f1}C_{HT} \quad (5)$$

The two Pt atoms in the HT dimer are equivalent, and deprotonation occurs to either one of the two axial water molecules. Since the deprotonated water molecule in the octahedral aquahydroxo complexes is generally not easily replaced by other ligands, the halide substitution would take place at the other water molecule on the opposite Pt atom, $Pt(N_3O)$. That is, the deprotonation [Equation (1)] and the first substitution reaction with halide [Equation (2)] would occur to the opposite axial sites of the Pt^{III} dimer.

Therefore, two reaction pathways shown in Scheme 2 should be considered under the present condition for the

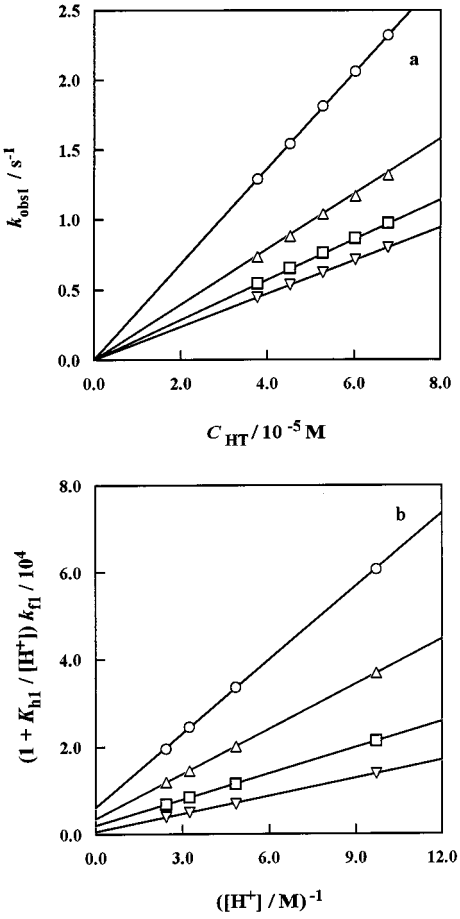

Figure 3. (a) The dependence of k_{obs1} on C_{Pt2} for the reaction of the HT dimer with bromide ion in acidic aqueous solution at 20 °C and I = 2.00 M. [H$^+$] = 0.103 (O); 0.206 (Δ); 0.309 (□); 0.412 (▽) M. $C_{Br^-} = 8.75\times10^{-7}$ M. (b) Plot of $(1 + K_{h1}/[H^+])k_{f1}$ against 1/[H$^+$] for the reaction of the HT dimer with bromide ion at 20 °C and I = 2.00 M; T = 25.0 (O); 20.0 (Δ); 15.0 (□); 10.6 (▽) °C

monohalo complex formation. For the reaction pathways in Scheme 2, the rate constant k_{obs1} is given by Equation (6).

$$k_{obs1} = \frac{k_1 + \frac{k_1^{\#}K_{h1}}{[H^+]}}{1 + \frac{K_{h1}}{[H^+]}} C_{HT} \quad (6)$$

Comparison of Equation (5) with Equation (6) gives Equation (7).

$$\left(1 + \frac{K_{h1}}{[H^+]}\right) k_{f1} = k_1 + \frac{k_1^{\#}K_{h1}}{[H^+]} \quad (7)$$

The plots of the left-hand side of Equation (7) against $[H^+]^{-1}$ were linear as shown in Figure 3 (b).

The values of k_1 and $k_1^{\#}$ were obtained by applying a nonlinear least-squares fitting to Equation (7), and are listed in Table 2. The K_{h1} values at each temperature are given as Supporting Information and were used for the calculation of k_1 and $k_1^{\#}$.

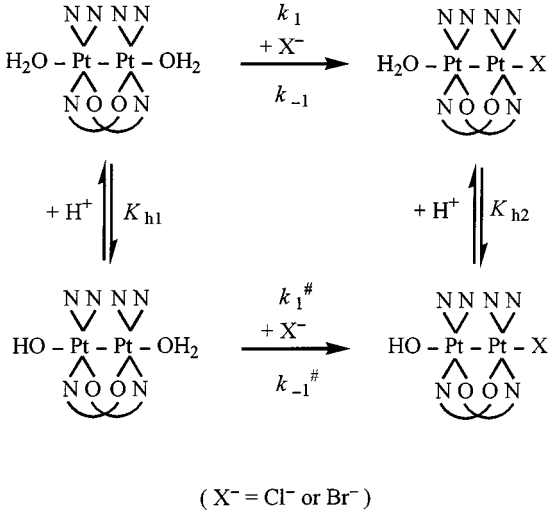

Scheme 2

Table 2. The rate constants (25 °C) and activation parameters for the first steps of the reactions of the HT dimer with halides

ligand	path	k [M^{-1}s^{-1}]	$\Delta H^{\#}$ [kJ mol^{-1}]	$\Delta S^{\#}$ [J mol^{-1}K^{-1}]
Cl$^-$	k_1	2.4×10^3 1.2×10^3 [a]	87.8±21.0	114±72
	$k_1^{\#}$	6.6×10^5 3.3×10^5 [a]	11.9±1.5	−93.7±5.3
Br$^-$	k_1	6.5×10^3 3.3×10^3 [a]	79.7±1.0	95.3±3.0
	$k_1^{\#}$	5.3×10^5 2.7×10^5 [a]	23.1±0.7	−57.9±2.0

[a] Statistical factor was taken into account (see text).

In the following discussion, half of k_1 was considered, since X$^-$ can replace both aqua ligands with an equal probability. Interestingly, the k_1 value for the reaction with Br$^-$ is larger than that with Cl$^-$; this relation is the same as that for the reactions of mononuclear Pt^{II} complexes, where the heavier halides with higher polarizability react faster. On the contrary, the $k_1^{\#}$ value is larger for Cl$^-$ than Br$^-$, which may reflect the decreased polarizability of the Pt(N$_3$O) in the HT dimer due to the deprotonation of the water molecule on the opposite axial site. We concluded that the ligand substitution rates on the axial sites of the HT dimer are sensitive to the nature of the ligands on the opposite axial site.

It is noteworthy that the rate constants k_1 and $k_1^{\#}$ in Table 2 are much larger than those for the direct substitution paths of the square planar Pt^{II} Werner-type complexes, which are of the order of 10^{-3} M^{-1}s^{-1}. A linear relationship was observed between $\Delta H^{\#}$ and $\Delta S^{\#}$ as shown in Figure SI-2 (Supporting Information, see footnote on the first page of this article), which suggests that both k_1 and $k_1^{\#}$ paths are via the same mechanism.[27,28]

For many octahedrally coordinated metal ions $[M(H_2O)_6^{n+}]$, substitution rate constants on the hexaaqua metal ions are smaller by 2−3 orders of magnitude than those of the corresponding pentaaquahydroxo metal ions $[M(H_2O)_5(OH)^{(n-1)+}]$.[29] The k_1 and $k_1^{\#}$ values in Table 2 show that the same tendency holds even through the present complexes having metal−metal bonds.

The values of k_1 and $k_1^{\#}$ in Table 2 are much larger than the rate constants of the axial ligand substitution (k_1 = 0.9 and 0.3 $M^{-1}s^{-1}$, k_2 = 0.8 and 0.4 $M^{-1}s^{-1}$ for X = Cl^- and Br^-, respectively) for the following $Pt^{III}-Pt^{III}$ system.[1]

$$Pt_2(\mu\text{-}PO_4H)_4(H_2O)_2^{2-} \underset{}{\overset{k_1}{\underset{+X^-}{\rightleftharpoons}}} Pt_2(\mu\text{-}PO_4H)_4X(H_2O)^{3-} \overset{k_2}{\underset{+X^-}{\rightleftharpoons}} Pt_2(\mu\text{-}PO_4H)_4X_2^{4-} \quad (8)$$

The large difference in the k_1 values would come from the difference of the bridging ligand, as well as the affinity difference of the halide ions for the positively charged amidate-bridged complex and for the negatively charged complex in Equation (8).

The effect of ion pairing was not observed for both reactions (2) and (3), in spite of the highly positive charge of the complexes (4+ or 3+). This is probably because the rate constants were measured at high ionic strength (2 M), where an ion-paring effect is attenuated, and the formal charge would be delocalized over the dinuclear complexes. The rate constant for reaction (2), k_{obs1}, was measured at low C_{HT} (10^{-4} M > C_{HT} >> C_X-).

Kinetics for the Formation of the Dihalo Complexes

Under the conditions of C_{HT} << C_X^- and $[H^+]$ = 0.11−1.3 M, the reaction of the HT dimer was biphasic as shown in Figure 4. The rate constant was calculated only for the slower reaction by assuming two consecutive first-order reactions.

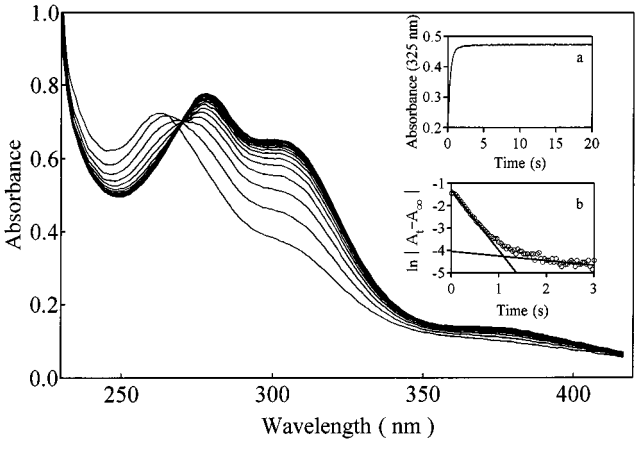

Figure 4. The UV/Vis spectra for the reaction of the HT dimer with chloride ion in acidic aqueous solution at 25 °C and I = 2.00 M. Measurement every 80 ms, C_{Cl^-} = 8.0×10^{-4} M, C_{HT} = 2.0×10^{-5} M, $[H^+]$ = 0.102 M. The inserted figure (a) shows the time dependence of the absorbance at 325 nm, and the semi-log plot (b) of the data in (a) shows clearly that the reaction is biphasic

The formation rate of the dihalo complex (Pt_2X_2) is expressed as Equation (9), where [HT−X] is the concentration of the monohalo-HT dimer.

$$d[Pt_2X_2] / dt = k_{obs2}[HT\text{-}X] \quad (9)$$

For the reaction with Cl^-, k_{obs2} was linear with respect to C_{Cl^-} at a given $[H^+]$ as shown in Figure 5 (a). The straight lines correspond to Equation (10), where k_{f2} and k_{d2} are the slope and the intercept in Figure 5 (a), respectively.

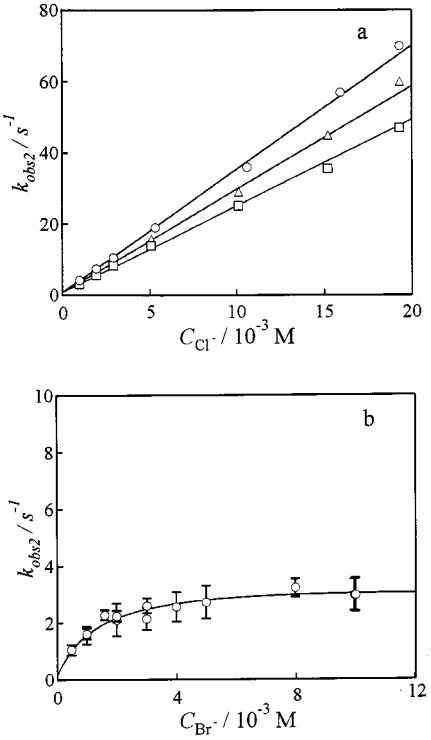

Figure 5. The dependence of k_{obs2} on C_X^- in acidic aqueous solution at 25 °C and I = 2.00 M. (a) for the reaction of the HT dimer with chloride ion, C_{HT} = 2.0×10^{-5} M, $[H^+]$ = 1.27 (□), 0.424 (Δ), 0.106 (O) M; (b) for the reaction of the HT dimer with bromide ion, C_{HT} = 2.0×10^{-5} or 4.0×10^{-5} M, $[H^+]$ = 0.4−1.6 M. The solid lines were drawn by applying a linear or non-linear least-squares fitting

$$k_{obs2} = k_{f2} C_{Cl^-} + k_{d2} \quad (10)$$

It is obvious from Figure 5a that k_{obs2} varies with $[H^+]$ in the same way as in Figure 3 (a), that is, k_{f2} in Equation (10) decreases with increasing $[H^+]$, whereas k_{d2} does not depend on $[H^+]$. For the second Cl^- substitution reaction, the reaction path in Scheme 3 was postulated, for which Equation (11) was derived.

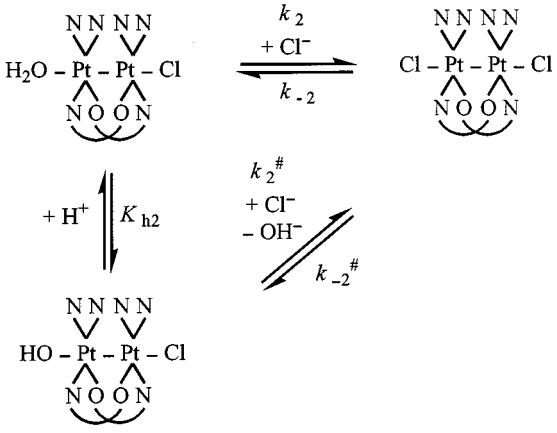

Scheme 3

$$k_{obs\,2} = \frac{k_2 + \frac{k_2^{\#} K_{h2}}{[H^+]}}{1 + \frac{K_{h2}}{[H^+]}} C_{Cl^-} + k_{-2} + \frac{k_{-2}^{\#} K_w}{[H^+]} \qquad (11)$$

The observed dependence of k_{f2} on $[H^+]$ corresponds to the coefficient of C_{Cl^-} in Equation (11). In Scheme 3, it was assumed that the coordinated OH^- is replaced by X^-. If the OH^- in the hydrolyzed species (the chlorohydroxo dimer in Scheme 3) is unreactive towards Cl^-, then $k_{obs2} = k_2[H^+][Cl^-]/([H^+] + K_{h2}) + k_{-2}$ is obtained. This equation does not correspond with the experimental observation that k_{obs2} decreases with increasing $[H^+]$. Thus, the $k_2^{\#}$ path, in which OH^- in the [HO−Pt−Pt−X] is replaced by X^-, must be involved in the HT + Cl^- system. This is unusual, considering the usual inertness of OH^- in $M(H_2O)_5(OH)^{(n-1)+}$. In HH α-pyridonate-dibridged complexes, HH-[Cl−Pt(N_2O_2)−Pt(N_4)−X], when X^- is changed from less donating NO_3^- to more donating Cl^-, the opposite (N_2O_2)Pt−Cl distance (236.0 pm → 245.5 pm) as well as the Pt−Pt length (262.4 pm → 263.7 pm) are elongated.[30] Such significant trans influence of Cl^- on the opposite axial ligand suggests that the Pt−OH distance in the HT-[HO−Pt−Pt−Cl] can be longer than usual, and OH^- in the HT-[HO−Pt−Pt−Cl] may be replaced by Cl^-. The third term in Equation (11) is negligible under the present conditions ($[H^+]$ = 0.11−1.3 M), that is, k_{d2} is virtually equal to k_{-2}.

The conditional formation constant (k_{f2}/k_{d2}) for the dichloro complex of the HT dimer can be calculated from the slope (k_{f2}) and the intercept (k_{d2}) at a given $[H^+]$. The obtained $\log(k_{f2}/k_{d2})$ value (3.64) at $[H^+]$ = 1.27 M agrees with $\log K_2^{Cl}$ listed in Table 1, within the experimental error.

On the other hand, for the reaction with Br^-, k_{obs2} increases linearly with $[Br^-]$ at lower $[Br^-]$, and at higher $[Br^-]$ it also increases linearly, but with a different slope as shown in Figure 5 (b). In both non-Werner Pt^{II} complexes and octahedral Pt^{IV} complexes, e.g., $Pt^{II}R_2S_2$ (R = Me, Ph; S = Me_2S, Me_2SO) or $Pt^{IV}Me_4(Me_2S)_2$, a dissociative mechanism has been proposed for the solvolysis reactions, and this is because of the strong *trans* labilizing effect of Me and Ph groups.[31−34] The trans effect is also observed through the Pt−Pt bond for the present HT dimer as mentioned above. It is reported that there is virtually no axial ligand on the Pt(N_4) in the HH pivalamidate-bridged Pt^{III} dimer with the alkyl ligand (R) on the Pt(N_2O_2), i.e., [Pt^{II}(N_4)−Pt^{IV}(N_2O_2)−R].[24] On the basis of these findings, it seems that reaction (3) proceeds also through a dissociative path via a coordinatively unsaturated complex as depicted in Scheme 4. It is also notable that k_{obs2} is almost independent of $[H^+]$. If the steady-state approximation is applied to the monohalo dimer without an axial ligand at the opposite site in Scheme 4, Equation (12a) involving the three terms is obtained. The first and second terms in Equation (12a) are related to the k_2 path, and the third is to the k_3 path. The $k_2^{\#}$ path in Scheme 3 is irrelevant in Scheme 4, since k_{obs2} does not vary with $[H^+]$ for the (HT + Br^-) system.

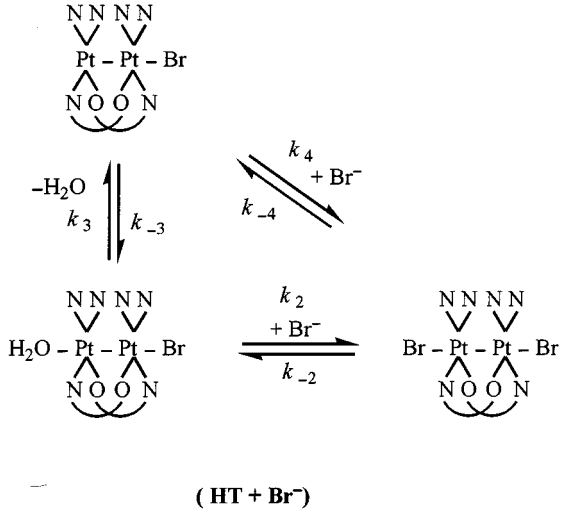

Scheme 4

$$k_{obs2} = k_2[Br^-] + k_{-2} + \frac{k_3 k_4 [Br^-] + k_{-3} k_{-4}}{k_{-3} + k_4 [Br^-]} \qquad (12a)$$

The following values were estimated from the data in Figure 5 (a, b) by applying a non-linear least-squares fitting to Equation (11) or Equation (12b) derived from Equation (12a), assuming that $k_{-2}^{\#} K_W/[H^+] = 0$ in Equation (11), and $k_{-2} = 0$ and $k_{-3}k_{-4}/k_4 = 0$ in Equation (12b): k_2 = 2490±40 $M^{-1}s^{-1}$, $k_2^{\#}K_{h2}$ = 115±5 s^{-1}, and k_{-2} = 0.59±0.38 s^{-1} for Figure 5 (a); k_2 = −25±29 $M^{-1}s^{-1}$, k_3 = 3.7±0.4 s^{-1}, and k_{-3}/k_4 = (1.4±0.2) ×10^{-3} M for Figure 5 (b) (k_2 could not be determined accurately because of the large error in k_{obs2}).

$$k_{obs2} = k_2[Br^-] + k_{-2} + \frac{k_{-3}[Br^-] + k_{-3}k_{-4}/k_4}{k_{-3}/k_4 + [Br^-]} \quad (12b)$$

The data in Figure 5 (b) were also analyzed by assuming a mechanism that involves ion pair formation. However, the fit was very poor, and the ratio of the resulting rate constants, k_2/k_{-2}, did not agree at all with K_2 obtained from the spectrophotometry, and so the ion pair formation is negligible under the present conditions.

The *trans* influence and/or the *trans* effect through the Pt−Pt bond seems to determine the reaction paths (see Schemes 3 and 4). In the aquachloro HT dimer, [H_2O−Pt−Pt−Cl], the axial aqua ligand is more acidic than that in the corresponding monobromo HT complex because of the weaker trans influence of chloride, but yet the trans effect of the axial chloride ligand is strong enough to replace the OH^- with Cl^- in the chlorohydroxo HT dimer, as is the case in Scheme 3. On the other hand, the increased *trans* influence and *trans* effect of the bromide lengthen and labilize the H_2O−Pt bond in the aquabromo HT complex, which promotes the dissociation of H_2O to produce the monohalo dimers without an axial ligand at the opposite site. This is the case in Scheme 4.

The mechanistic difference between the HT-[H_2O−Pt−Pt−Cl] and HT-[H_2O−Pt−Pt−Br] systems would reflect the relative extent of the electron donor ability of Cl^- and Br^-, that is, softer Br^- donates more electrons to the H_2O−Pt atom through the Pt−Pt bond, which enhances more the electron delocalization in the dimer (such as [H_2O−Pt^{II}−Pt^{IV}−Br]).

Conclusion

The first deprotonation occurs on one of the water molecules on the two equivalent Pt atoms and the first nucleophilic substitution with X^- occurs to the other Pt atom in the HT dimer. The formation of the HT dichloro complex from the aquachloro complex proceeds through two pathways: by a direct substitution of the aqua ligand and by a path involving OH^- substitution in the chlorohydroxo complex. The formation of the dibromo complex from the aquabromo complex, on the other hand, proceeds through a dissociative path by a coordinatively unsaturated complex as well as through a direct substitution path. The ligand substitution rates on the axial sites of the HT dimer are very sensitive to the nature of the ligands on the opposite axial sites. The mechanistic difference of the ligand substitution on the aquahalo complexes is reasonably explained by the different electron donor ability of Cl^- and Br^-.

Experimental Section

Reagents: The *cis*-[$PtCl_2(NH_3)_2$] (N.E. Chemcat) was purchased and was used without purification. Reagent grade α-pyridone (Kanto Chemical Co. Inc., Tokyo) was recrystallized once from benzene. Sodium chloride (99.99%, Kanto), sodium bromide (99.99%, Aldrich), and perchloric acid (60% UGR for trace analysis, Kanto) were used as received. Sodium perchlorate was prepared and purified according to the literature.[35] Head-to-tail [$(NO_3)Pt(NH_3)_2(\mu\text{-}C_5H_4NO)_2Pt(NH_3)_2(NO_3)](NO_3)_2\cdot 0.5H_2O$ (HT isomer) were prepared according to the literature method.[4]

Measurements: Ionic strength was maintained at 2.00 M with perchloric acid and sodium perchlorate. All the sample solutions were prepared by using water twice distilled just before measurement. Spectrophotometric measurements were performed with a rapid-scan/stopped-flow spectrophotometer USP-500 (Unisoku Scientific Instruments, Osaka) and spectrophotometers UV-160A (Shimadzu, Kyoto), UV-2200 (Shimadzu), and UV-2400 (Shimadzu). The NMR spectra were recorded on a JEOL Lambda 270 spectrometer, operating at 270 MHz for ^1H. Chemical Shifts are reported relative to TMS (tetramethylammonium perchlorate, 3.190 ppm to TMS). Under the present experimental conditions with the concentration of sodium halide (C_{X^-}, X^- = Cl^- or Br^-) in large excess over that of the HT dimer (C_{HT}), the reaction was biphasic as shown in Figure 4, and is expressed by the equation: $A_t = A_e + \alpha\exp(-k_{obs1}t) + \beta\exp(-k_{obs2}t)$, where A_t and A_e are the absorbances at time t and ∞, respectively, and α and β are composite parameters.[28] Though it is possible to estimate k_{obs1} and k_{obs2} simultaneously under the condition $C_{HT} << C_{X^-}$, k_{obs1} was determined independently under the conditions $C_{HT} >> C_{X^-}$ in order to obtain more accurate values. Rate constants were measured by monitoring the absorbance change at 265 nm for the reaction of the HT dimer with Cl^-, and at 270 nm with Br^- for k_{obs1}, at 250 nm for the reaction of the HT dimer with Cl^-, and at 265 or 350 nm for the reaction of the HT dimer with Br^- for k_{obs2}, as a function of time after mixing the solutions of the dimer and sodium halide. For the reaction with Br^-, the dependence of k_{obs2} on C_{Br^-} was not straightforward (see Results). The acid dissociation constant (K_{h1}) of the HT dimer and the formation constants (K_1^X and K_2^X) of the monohalo and the dihalo complexes were determined spectrophotometrically under the following conditions: C_{HT} = (5−6) $\times 10^{-5}$ M, $[H^+] = 1.00\times 10^{-3}$ to 0.501 M for K_{h1}; $C_{HT} = 2.48\times 10^{-5}$ M, $[H^+]$ = 1.27 M, $C_{Cl^-} = 0-1.3\times 10^{-2}$ M for K_1^{Cl} and K_2^{Cl}; $C_{HT} = 2\times 10^{-5}$ M, $[H^+]$ = 1.27 M, $C_{Br^-} = (0-4)\times 10^{-2}$ M for K_1^{Br} and K_2^{Br}. The values of K_2^{Br} was determined by using the spectroscopic data obtained only for $C_{Br^-} < 1.2\times 10^{-2}$ M, since the spectra changed differently with a different isosbestic point at higher C_{Br^-}, probably due to the reduction of the Pt^{III} dimers by water.[19]

[1] R. El-Mehdawi, S. A. Bryan, D. M. Roundhill, *J. Am. Chem. Soc.* **1985**, *107*, 6282 and references cited therein.
[2] S. Bryan, M. K. Dickson, D. M. Roundhill, *Inorg. Chem.* **1987**, *26*, 3878, and references cited therein.
[3] R. Faggiani, B. Lippert, C. J. L. Lock, R. A. Speranzini, *J. Am. Chem. Soc.* **1981**, *103*, 1111.
[4] L. S. Hollis, S. J. Lippard, *Inorg. Chem.* **1983**, *22*, 2605.
[5] L. S. Hollis, M. M. Roberts, S. J. Lippard, *Inorg. Chem.* **1983**, *22*, 3637.
[6] T. V. O'Halloran, M. M. Roberts, S. J. Lippard, *Inorg. Chem.* **1986**, *25*, 957.
[7] B. Lippert, H. Schoellhorn, U. Thewalt, *Inorg. Chem.* **1986**, *25*, 407.
[8] H. Schoellhorn, P. Eisenmann, U. Thewalt, B. Lippert, *Inorg. Chem.* **1986**, *25*, 3384.
[9] B. Lippert, H. Schoellhorn, U. Thewalt, *J. Am. Chem. Soc.* **1986**, *108*, 525.

[10] [10a] T. Abe, H. Moriyama, K. Matsumoto, *Chem. Lett.* **1989**, 1857. – [10b] T. Abe, H. Moriyama, K. Matsumoto, *Inorg. Chem.* **1991**, *30*, 4198.
[11] J. K. Barton, H. N. Rabinowitz, D. J. Szalda, S. J. Lippard, *J. Am. Chem. Soc.* **1977**, *99*, 2827.
[12] J. K. Barton, D. J. Szalda, H. N. Rabinowitz, J. V. Waszczak, S. J. Lippard, *J. Am. Chem. Soc.* **1978**, *100*, 1434.
[13] J. K. Barton, C. Caravana, S. J. Lippard, *J. Am. Chem. Soc.* **1979**, *101*, 7269.
[14] L. S. Hollis, S. J. Lippard, *J. Am. Chem. Soc.* **1981**, *103*, 1230.
[15] K. Matsumoto, K. Fuwa, *J. Am. Chem. Soc.* **1982**, *104*, 897.
[16] K. Matsumoto, H. Takahashi, K. Fuwa, *Inorg. Chem.* **1983**, *22*, 4086.
[17] K. Matsumoto, K. Fuwa, *Chem. Lett.* **1984**, *569*.
[18] K. Matsumoto, K. Fuwa, *J. Am. Chem. Soc.* **1984**, *106*, 2049.
[19] K. Matsumoto, *Chem. Lett.* **1984**, 2061.
[20] K. Matsumoto, *Bull. Chem. Soc. Jpn.* **1985**, *58*, 651.
[21] E. S. Peterson, D. P. Bancroft, D. Min, F. A. Cotton, E. A. Abbott, *Inorg. Chem.* **1990**, *29*, 229.
[22] T. V. O′Halloran, S. J. Lippard, *Inorg. Chem.* **1989**, *28*, 1289.
[23] K. Matsumoto, K. Mizuno, T. Abe, J. Kinoshita, H. Shimura, *Chem. Lett.* **1994**, 1325.
[24] K. Matsumoto, Y. Nagai, J. Matsunami, K. Mizuno, T. Abe, R. Somazawa, J. Kinoshita, H. Shimura, *J. Am. Chem. Soc.* **1998**, *120*, 2900.
[25] K. Sakai, Y. Tsuchiya, T. Tsubomura, *Technol. Rep. Seikei Univ.* **1992**, *54*, 77.
[26] R. B. Jordan, *Reaction Mechanisms of Inorganic and Organometallic Systems*, Oxford, **1991**, p. 77−80.
[27] C. P. Brink, A. L. Crumbliss, *Inorg. Chem.* **1984**, *23*, 4708.
[28] R. G. Wilkins, *Kinetics and Mechanism of Reactions of Transition Metal Complexes*, 2nd ed., VCH, **1991**.
[29] A. E. Martell (Ed.), *Coordination Chemistry*; Vol. 2, ACS Monogr. No. 174, **1978**, p. 106.
[30] K. Sakai, Y. Tanaka, Y. Tsuchiya, K. Hirata, T. Tsubomura, S. Iijima, A. Bhattacharjee, *J. Am. Chem. Soc.* **1998**, *120*, 8366.
[31] R. Romeo, *Comments Inorg. Chem.* **1990**, *11*, 21.
[32] G. Alibrandi, L. M. Scolaro, R. Romeo, *Inorg. Chem.* **1991**, *30*, 4007.
[33] K. Nakayama, Y. Kondo, K. Ishihara, *Can. J. Chem.* **1998**, *76*, 62.
[34] J. D. Atwood, *Inorganic and Organometallic Reaction Mechanisms*, 2nd ed., VCH-Verlagsgesellschaft, Weinheim, **1997**, p. 59.
[35] S. Funahashi, K. Haraguchi, M. Tanaka, *Inorg. Chem.* **1977**, *16*, 1349.

Received January 6, 2001
[I01018]